**Stochastic Optimization of Wind Turbine Power Factor Using Stochastic Model of Wind Power**

Chen, Peiyuan; Siano, Pierluigi; Bak-Jensen, Birgitte; Chen, Zhe

# Stochastic Optimization of Wind Turbine Power Factor Using Stochastic Model of Wind Power

Peiyuan Chen, *Member, IEEE*, Pierluigi Siano, Birgitte Bak-Jensen, *Member, IEEE*, and Zhe Chen,
*Senior Member, IEEE*

*Abstract*-- **This paper proposes a stochastic optimization algorithm that aims to minimize the expectation of the system power losses by controlling wind turbine (WT) power factors. This objective of the optimization is subject to the probability constraints of bus voltage and line current requirements. The optimization algorithm utilizes the stochastic models of wind power generation (WPG) and load demand to take into account their stochastic variation. The stochastic model of WPG is developed on the basis of a limited autoregressive integrated moving average (LARIMA) model by introducing a cross-correlation structure to the LARIMA model.**

**The proposed stochastic optimization is carried out on a 69-bus distribution system. Simulation results confirm that, under various combinations of WPG and load demand, the system power losses are considerably reduced with the optimal setting of WT power factor as compared to the case with unity power factor. Furthermore, an economic evaluation is carried out to quantify the value of power loss reduction. It is demonstrated that not only network operators but also WT owners can benefit from the optimal power factor setting, as WT owners can pay a much lower energy transfer fee to the network operators.**

***Index Terms*--Correlation, Monte Carlo, power factor, stochastic optimization, time series, wind power generation.**

## I. INTRODUCTION

WIND power generation (WPG) has been the focus in developing modern electrical generation technologies [1]. In the European Union in 2008, WPG accounted for 36% of all new electricity generating capacity, exceeding all other generation technologies [2]. In order to fully utilize potential benefits and to minimize adverse impacts of WPG, many research efforts have been devoted to exploring the technical and economic contribution of wind power in power systems [3]. These studies include system planning, daily operation and electricity market of wind power [3].

Due to their dispersed locations in distribution systems, wind turbines (WTs) can be used to provide local reactive power consumption. This decreases reactive power flow from the main grid and thus increases active power transfer capacity of substation transformers. The reduced reactive power flow also brings down active and reactive power losses in distribution systems. The reduction of active power losses cuts down the network operating costs without extra investment. Furthermore, the increase in transformer power transfer capacity may defer network expansion. All these benefits can be obtained by network operators if they have access to the power factor setting of WTs. However, this is usually not the case if network operators are not the owner of the WTs. On the other hand, the power factor setting of WTs are accessible to WT owners, although they may not be willing to change the setting unless there is an economic incentive to do so. In other words, WT owners may be motivated to change the power factor setting upon the request of network operators, if the network operators share the obtained economic benefits with WT owners. Thus, for the sake of mutual benefits, it is necessary to estimate the power losses in advance that may be reduced by WT power factor setting and to quantify corresponding economic benefits in the long run.

In order to evaluate such economic benefits, the capability of WTs to provide reactive power generation should be evaluated first. In other words, the power factors of WTs should be set at certain optimal values instead of unity value in order to minimize power losses. Nevertheless, this optimal setting is strongly affected by the system WPG and load demand, both of which vary stochastically. This indicates that the optimal power factor setting needs to take into account the stochastic processes of WPG and load demand. Thus, a stochastic optimization algorithm based on stochastic programming can be used to find the optimal power factor setting that adapts to the stochastic behavior of system power flow [4]-[6]. Such a stochastic optimization entails stochastic modeling of WPG and load demand.

As discussed in [7], the hourly load demand usually has a Gaussian distribution. Thus, the load demand can be modeled by a multivariate Gaussian distribution or a standard autoregressive moving-average (ARMA) process [7]. In contrast, WPG is a non-Gaussian and non-stationary stochastic process, which makes it more challenging to apply standard multivariate probability distributions or ARMA models.

In the literature, stochastic models of WPG are developed on the basis of an ARMA process [8]-[11] or a discrete Markov process [12]-[14]. These models capture the chronological characteristics of WPG adequately. However, these stochastic wind power models are developed for simulating WPG from a single wind farm. The same

techniques cannot be directly applied to the modeling of WPG from several wind farms as WPGs from different wind farms may be correlated with each other due to similar wind conditions.

Nevertheless, the modeling of such a cross-correlation among WPGs from these wind farms is of great importance as it significantly affects the probability distribution of the total WPG in a power system [15]. In the literature, the cross-correlation model of multiple WPG process is implemented through a trial-and-error approach [16], [17], or a Gaussian copula [18]. Both approaches model the cross-correlation of wind speed at adjacent areas where wind farms are located. Then, the correlated wind speed is transformed through a wind farm power curve to obtain correlated WPG.

The trial-and-error approach implemented in [16] and [17] considers only the correlation coefficient at time-lag zero. Correlation coefficients at higher time lags are not addressed or properly modeled. Furthermore, the approach makes the implementation of the model very difficult when three or more WPG processes are involved. On the other hand, the Gaussian copula approach proposed in [18] is suitable for modeling the cross-correlation of multivariate stochastic variables. However, WPG is a stochastic process, of which the modeling of autocorrelation is very important. Therefore, the Gaussian copula approach is not appropriate as it is not able to model the autocorrelation of WPG.

This paper develops a multivariate stochastic wind power model that includes both the autocorrelation and cross-correlation structure of WPG. The cross-correlation structure considers not only the correlation coefficient at time-lag zero, but also the ones at higher time lags. Then, the multivariate stochastic wind power model is incorporated into a stochastic optimization algorithm, which minimizes the expectation of system power losses by setting the optimal power factor values of WTs. In the end, an economic evaluation of power loss reduction is provided to demonstrate the benefits obtained by both network operators and WT owners.

The rest of the paper is organized as follows. Section II develops the multivariate stochastic wind power model. Section III presents the stochastic optimization algorithm for WT power factor setting. Section IV describes the case-study system based on a 69-bus distribution network. Section V provides the optimization results of WT power factor setting and evaluates corresponding economic benefits. Concluding remarks and future works are stated in Section VI.

## II. MULTIVARIATE STOCHASTIC WIND POWER MODEL

This section first discusses two types of correlation modeling for WPGs from adjacent wind farms. Then, a multivariate time series model is introduced and applied to the modeling of two correlated WPGs. Finally, the multivariate wind power model is validated against measurements.

### A. Autocorrelation and Cross-Correlation

WPG from a wind farm is a stochastic process, which possess a strong temporal correlation. Furthermore, WPGs from adjacent wind farms are cross-correlated due to similar wind conditions. Thus, the correlation model of WPG should comprise two parts: autocorrelation and cross-correlation.

The autocorrelation of WPG is the correlation of wind power in time. The theoretical autocorrelation coefficient of a random process is usually not known, but can be estimated from an observed time series $y(t)$ by the sample autocorrelation coefficient. The sample autocorrelation coefficient at time-lag $k$ is calculated by [19]:

$$\hat{\rho}_Y(k) = \frac{\frac{1}{N-k}\sum_{i=1}^{N-k}\left[y(i)y(i+k)\right] - m^2}{s^2}, \text{ for } k = 0,1,\dots N-1 \quad (1)$$

where $m$ and $s^2$ are the sample mean and sample variance of the observed time series $y(t)$, respectively; N is the length of the time series $y(t)$.

On the other hand, the cross-correlation of WPG is the correlation of wind power among multiple wind farms (or WTs) in space. Assume that there are $n$ wind farms and that their observed wind power time series are denoted by the vector $\mathbf{y(t)} = [y_1(t), y_2(t), \dots, y_n(t)]^T$. Then, the sample cross-covariance matrix at time-lag $k$ can be calculated by [19]:

$$\hat{\mathbf{\Gamma}}(k) = \begin{bmatrix} \hat{\gamma}_{11}(k) & \hat{\gamma}_{12}(k) & \cdots & \hat{\gamma}_{1n}(k) \\ \hat{\gamma}_{21}(k) & \hat{\gamma}_{22}(k) & \cdots & \hat{\gamma}_{2n}(k) \\ \cdots & \cdots & \cdots & \cdots \\ \hat{\gamma}_{n1}(k) & \hat{\gamma}_{n2}(k) & \cdots & \hat{\gamma}_{nn}(k) \end{bmatrix}, \quad (2)$$

where the sample cross-covariance of the wind power time series between wind farm $i$ and wind farm $j$ at time-lag $k$ is:

$$\hat{\gamma}_{ij}(k) = \frac{1}{N-k}\sum_{t=1}^{N}\left[\left(y_i(t)-m_i\right)\left(y_j(t+k)-m_j\right)\right], \quad (3)$$

where $m_i$ is the sample mean of time series $y_i(t)$. Consequently, the corresponding sample cross-correlation coefficient $\hat{\rho}_{ij}$ is:

$$\hat{\rho}_{ij}(k) = \frac{\hat{\gamma}_{ij}(k)}{\sqrt{\hat{\gamma}_{ii}(0)\hat{\gamma}_{jj}(0)}}. \quad (4)$$

For modeling WPG from a single wind farm, only autocorrelation needs to be considered. For example, for modeling the WPG of the Nysted offshore wind farm (Denmark), autocorrelation is captured by the LARIMA model adequately as shown in [11]. However, in the case of multiple wind farms in a power system, both autocorrelation and cross-correlation should be taken into account. This calls for a multivariate time series model, which is introduced in the following subsection.

## B. Multivariate Time Series Model

In order to describe the relationship among several time series variables, multivariate time series models can be applied. Multivariate time series models are also referred to as vector time series models [19]. The multivariate-ARIMA($p, d, q$) model of $n$ nonstationary random processes, $Z_1(t), Z_2(t), \ldots$, and $Z_n(t)$, is expressed as [19]:

$$\left(\mathbf{I}-\mathbf{\Phi_p}B\right)\mathbf{D}(B)\mathbf{Z}(t) = \mathbf{\theta_0} + \left(\mathbf{I}-\mathbf{\Theta_p}B\right)\mathbf{a}(t) \qquad (5)$$

where $\mathbf{I}$ is an $n \times n$ identity matrix; the autoregressive (AR) coefficients $\mathbf{\Phi_p} = \{\varphi_{ij}\}$ is a $p \times p$ matrix and $p$ is the order of AR processes; the moving average (MA) coefficients $\mathbf{\Theta_q} = \{\theta_{ij}\}$ is a $q \times q$ matrix and $q$ is the order of MA processes; the differencing operator $\mathbf{D}(B) = \mathrm{diag}[(1 - B)^{d_1}, \ldots, (1 - B)^{d_n}]$ is an $n \times n$ diagonal matrix and $(d_1, \ldots, d_n)$ is a set of nonnegative integers; the multivariate time series $\mathbf{Z}(t) = [Z_1(t), Z_2(t), \ldots, Z_n(t)]^T$ is an $n \times 1$ vector; $\mathbf{\theta_0}$ is referred to as the deterministic trend term; the multivariate Gaussian white process $\mathbf{a}(t) = [a_1(t), a_2(t), \ldots, a_n(t)]^T$ has zero mean and an $n \times n$ covariance matrix $\mathbf{\Sigma_a}$.

## C. Modeling of Correlated Wind Power Generation

Hourly wind power data are measured from the Nysted offshore wind farm in Denmark from Jan. 1 to Dec. 31, 2005. The wind farm has 72 fixed-speed wind turbines, each rated 2.3 MW. Thus, the total capacity of the wind farm is 165.6 MW. The measurements are obtained from two parts of the wind farm. Each part has a total capacity of 82.8 MW. As a result, the two hourly measured wind power time series of one-year length are available for model development.

Following the same modeling procedures described in [11], WPG from an individual part of the wind farm can be modeled by a LARIMA(0,1,1) model. However, in order to model the cross-correlation of the WPGs between the two parts of the wind farm, the multivariate time series model should be applied. Such a multivariate time series model can be developed according to (5) with a model structure based on the LARIMA(0,1,1) model. This leads to a bivariate-LARIMA(0,1,1) model as shown in Fig. 1.
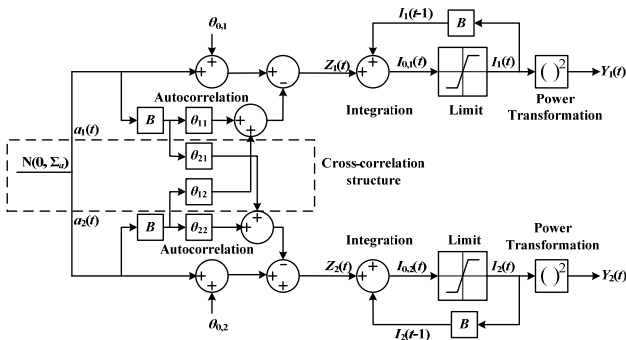


Fig. 1. Block diagram of the bivariate-LARIMA(0,1,1) model.

The bivariate-LARIMA model is composed of integration, limiter, power transformation, autocorrelation and cross-correlation. Such a bivariate-LARIMA model is more sophisticated than the LARIMA model developed in [11] as the bivariate-LARIMA model is able to simulate the cross-correlation between two wind power time series. The cross-correlation structure is composed of two parts: 1) a bivariate-Gaussian white noise with the covariance matrix $\mathbf{\Sigma_a}$, and 2) the cross-coupling of the white noise at time-lag one with weights of $\theta_{12}$ and $\theta_{21}$.

The mathematical formulation of the bivariate-LARIMA(0,1,1) model is summarized from (6)-(10). The corresponding model parameters are summarized in the Appendix.

$$\begin{bmatrix} Z_1(t) \\ Z_2(t) \end{bmatrix} = \begin{bmatrix} \theta_{0,1} \\ \theta_{0,2} \end{bmatrix} + \left\{ \begin{bmatrix} 1 & 0 \\ 0 & 1 \end{bmatrix} - \begin{bmatrix} \theta_{11} & \theta_{12} \\ \theta_{21} & \theta_{22} \end{bmatrix} B \right\} \begin{bmatrix} a_1(t) \\ a_2(t) \end{bmatrix}, \qquad (6)$$

$$\begin{bmatrix} Z_1(t) \\ Z_2(t) \end{bmatrix} = \begin{bmatrix} I_{0,1}(t) - I_1(t-1) \\ I_{0,2}(t) - I_2(t-1) \end{bmatrix}, \qquad (7)$$

$$I_1(t) = \begin{cases} \mathrm{I_{max}}, & I_{0,1}(t) > \mathrm{I_{max}} \\ I_{0,1}(t), & \mathrm{I_{min}} \le I_{0,1}(t) \le \mathrm{I_{max}} \\ \mathrm{I_{min}}, & I_{0,1}(t) < \mathrm{I_{min}} \end{cases}, \qquad (8)$$

$$I_2(t) = \begin{cases} \mathrm{I_{max}}, & I_{0,2}(t) > \mathrm{I_{max}} \\ I_{0,2}(t), & \mathrm{I_{min}} \le I_{0,2}(t) \le \mathrm{I_{max}} \\ \mathrm{I_{min}}, & I_{0,2}(t) < \mathrm{I_{min}} \end{cases}, \qquad (9)$$

$$\begin{bmatrix} Y_1(t) \\ Y_2(t) \end{bmatrix} = \begin{bmatrix} I_1^2(t) \\ I_2^2(t) \end{bmatrix}. \qquad (10)$$

where $\theta_{0,1}$ is the mean of the stochastic process $Z_1(t)$ and $\theta_{0,2}$ is the mean of the stochastic process $Z_2(t)$. $\theta_{11}$ is the weight for the autocorrelation of $Z_1$ and $\theta_{22}$ is the weight for the autocorrelation of $Z_2(t)$. $a_1(t)$ and $a_2(t)$ are the two correlated Gaussian white noise with zero means and the covariance matrix $\mathbf{\Sigma_a}$. $I_1(t)$ and $I_2(t)$ are the square-root of the simulated wind power $Y_1(t)$ and $Y_2(t)$, respectively. $I_{0,1}(t)$ and $I_{0,2}(t)$ are $I_1(t)$ and $I_2(t)$ before the limiter operation, respectively.

## D. Model Validation

In order to validate the bivariate-LARIMA(0,1,1) model, the two simulated time series ($Y_1(t)$ and $Y_2(t)$) of ten-year length (87600 data points) from the model are compared to the corresponding measurements ($y_1(t)$ and $y_2(t)$). The comparison is carried out in terms of sample autocorrelation coefficient, partial-autocorrelation coefficient, cross-correlation coefficient, and probability distribution [19]. Partial-autocorrelation coefficient describes the autocorrelation between $Y(t)$ and $Y(t+k)$ when the mutual linear dependency of $Y(t+1), Y(t+2), \ldots, Y(t+k-1)$ is removed [11].

Fig. 2 (a) shows the sample autocorrelation coefficients of the sum of the simulated time series ($Y_1(t) + Y_2(t)$), as well as the sum of the measured time series ($y_1(t) + y_2(t)$). Fig. 2 (b) shows the corresponding sample partial-autocorrelation coefficients. The results show a good fit in autocorrelation and partial-autocorrelation between the bivariate-LARIMA model and the measurements. The sample partial-autocorrelation goes to zero for time lags larger than three.

Fig. 2 (c) compares the sample cross-correlation coefficients of the simulated time series and the measured time series. The match in cross-correlation coefficients indicates that the proposed cross-correlation structure is sufficient to model the interdependence of the two parts of the wind farm. Furthermore, it is noted that the cross-correlation between the two parts of the wind farm is as high as their autocorrelation. It is worth pointing out that unlike autocorrelation, the values of cross-correlation are usually not symmetrical at the two sides of time-lag 0. Thus, both sides of the cross-correlation should be evaluated. However, in this case, the values of the cross-correlation at the two sides are very close, which is reasonable as it is between two parts of a wind farm. Thus, only one side of the cross-correlation is shown in Fig. 2 (c).
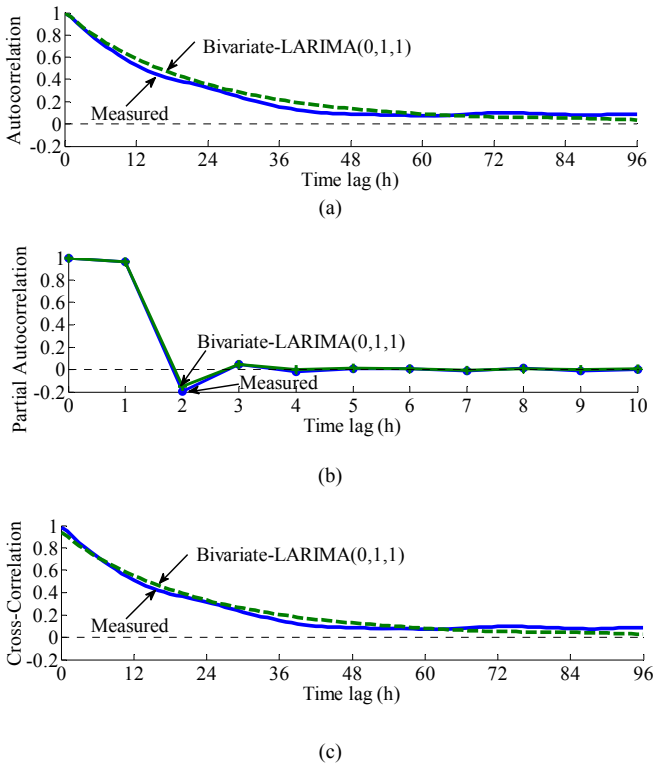


Fig. 2. Bivariate-LARIMA(0,1,1) model (dashed) versus measurements (solid): (a) Sample autocorrelation, (b) partial-autocorrelation, and (c) cross-correlation coefficients.

Fig. 3 compares the probability distribution of the sum of the simulated time series ($Y_1(t) + Y_2(t)$) with the measurements by using a quantile-quantile plot. If the simulated time series and the measured time series have the same probability distribution, then their quantile-quantile plot follows a straight line with a unit slope. Fig. 3 shows that the probability distribution of the model fits that of the measurements adequately.
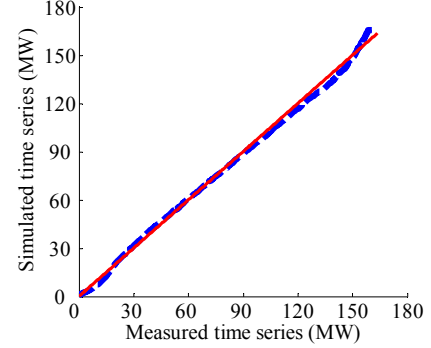


Fig. 3. Quantile-Quantile plot of the simulated time series from the bivariate-LARIMA(0,1,1) model against the measured time series (dashed), and straight line with unit slope (solid).

In fact, the cross-correlation of multivariate time series has a significant impact on the probability distribution of the sum of the multivariate time series. In order to demonstrate this, Fig. 4 shows the histograms of the probability distribution of the sum of two time series that are fully correlated, strongly correlated, weakly correlated and uncorrelated.
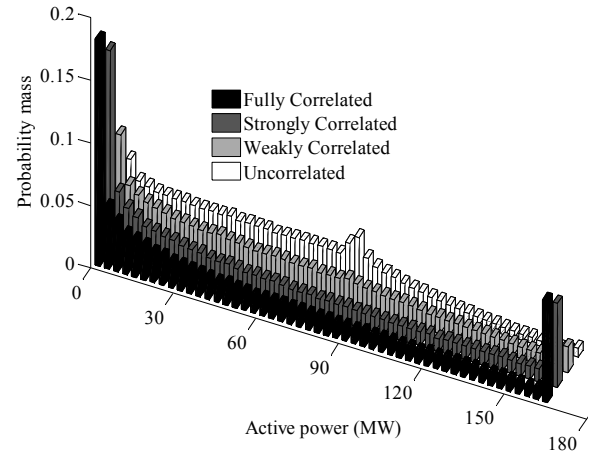


Fig. 4. Histogram of the probability mass of the sum of two time series when they are fully correlated, strongly correlated, weakly correlated and uncorrelated.

The two fully-correlated time series are identical to each other. The strongly correlated time series correspond to the two simulated time series ($Y_1(t)$ and $Y_2(t)$) as for Fig. 2 and Fig. 3. The weakly correlated time series are also simulated from the bivariate-LARIMA(0,1,1) model. However, the cross-correlation values (off-diagonal elements) of the covariance matrix $\Sigma_a$ of the white noise are one-tenth the values of the covariance matrix for the strongly correlated case (see (17)). The uncorrelated time series are simulated using the LARIMA model without the cross-correlation

structure. Fig. 4 shows a clear trend of the probability distribution when the cross-correlation between the two time series varies from full correlation to no correlation. The probability mass concentrates on the two ends of the distribution when the cross-correlation is strong. Whereas the probability mass moves to the center of the distribution when the cross-correlation is weak. In other words, a weak cross-correlation smoothens out the probability distribution of the total WPG. It is also worth pointing out that the mean values of the total WPG are identical for the four types of cross-correlation.

In summary, the bivariate-LARIMA(0,1,1) model captures the autocorrelation, the partial-autocorrelation, the cross-correlation and the probability distribution of the two measured wind power time series adequately. It is also demonstrated that the modeling of cross-correlation is of great importance as it strongly influences the probability distribution of the total WPG in a power system. Although the illustration is based on bivariate time series, the extension of the model to multivariate time series is mathematically straightforward. In the *n*-variate case, the cross-correlation structure shown in Fig. 1 is more complex, with an $n \times n$ covariance matrix of the white noise and an $n \times n$ matrix of the parameter $\boldsymbol{\theta}_1$.

## III. Stochastic Optimization of Wind Turbine Power Factor

This section illustrates the stochastic optimization algorithm used to design the power factor setting of WTs by taking into account the stochastic behavior of WPG and load demand.

Normally, grid-connected WTs are controlled to have a unity power factor. For fixed-speed WTs without power-electronic controllers, unity power factor is achieved by switching on/off capacitor banks. For variable-speed WTs with power-electronic controllers, unity power factor can be obtained by controlling the grid-side voltage source converter. There are several reasons to set WT power factor to unity. First, a unity power factor minimizes current flow and thus converter losses. Second, active power transfer capacity is maximized if there is no reactive power flow through the converter. However, from the network's perspective, WT power factor can be designed to minimize the power losses of the network. The reduced power losses lower the network operating cost for network operators.

Normally, such a loss minimization issue can be formulated and solved under the framework of a standard optimal power flow problem [20], [21]. However, in this case, both WPG and load are modeled by continuous stochastic processes, not by discrete probability masses as in [21]. Thus, a standard optimal power flow algorithm [20] cannot be directly adopted. Furthermore, as will be discussed later, probabilistic constraints of bus voltage and line current are implemented in the algorithm. This makes it even more difficult to apply the standard optimal power flow algorithm.

Therefore, a stochastic optimization based on Monte Carlo simulation is adopted to minimize the expectation of system power losses. In order to account for the seasonal variation, the optimization process is divided into four main periods, which are a summer weekday, a summer-weekend day, a winter weekday and a winter-weekend day. To take into consideration the diurnal period, each period is further grouped into 24 hours. Therefore, for each of the four periods, the objective of the stochastic optimization is to minimize the expectation of the total active power losses of the network at hour $t$, $P_L^t$, with respect to the power factor angle $\boldsymbol{\varphi}^t$ of WTs:

$$\min \mathrm{E}\left[P_L^t\left(\boldsymbol{\varphi}^t, \mathbf{P}_{WT}^t, \mathbf{P}_D^t\right)\right], \qquad \text{for } t = 1, 2, ..., 24, \qquad (11)$$

where E[ ] is to take the expectation of; $\boldsymbol{\varphi} = [\varphi_1, \varphi_2, ..., \varphi_n]$ is the vector of WT power factor angle; $n$ is the total number of WTs; $\mathbf{P}_{WT}^t$ is the vector of active WPG at hour $t$; $\mathbf{P}_D^t$ is the vector of active load demand at hour $t$. The load power factor is assumed constant at each bus.

$\boldsymbol{\varphi}^t$ consists of $n$ deterministic variables, while $\mathbf{P}_{WT}^t$ contains $n$ stochastic processes and $\mathbf{P}_D^t$ contains $d$ stochastic processes. As $P_L^t$ is a function of $\mathbf{P}_{WT}^t$ and $\mathbf{P}_D^t$, $P_L^t$ is also a stochastic variable. However, due to the non-Gaussian distribution of $\mathbf{P}_{WT}^t$ and the nonlinear loss function $P_L^t(\ )$, it is not straightforward to evaluate the expectation of $P_L^t$ analytically. Therefore, Monte Carlo simulations are adopted to evaluate the objective function (11). Such a Monte Carlo simulation calls for stochastic models of WPG and load demand.

The above objective function is subject to the following constraints:

$$\varphi_{\min} \le \varphi_i^t \le \varphi_{\max}, \qquad \text{for } i = 1, 2, ..., n, \qquad (12)$$

$$\mathrm{P}\left(V_j^t > V_{\max}\right) \le 2.5\%, \qquad \text{for } j = 1, 2, ..., J, \qquad (13)$$

$$\mathrm{P}\left(V_j^t < V_{\min}\right) \le 2.5\%, \qquad \text{for } j = 1, 2, ..., J, \qquad (14)$$

$$\mathrm{P}\left(I_k^t > I_{k,\max}\right) \le 5\%, \qquad \text{for } k = 1, 2, ..., K. \qquad (15)$$

where P( ) denotes the probability of; J is the total number of buses and K is the total number of branches. Equation (12) sets the lower ($\varphi_{\min}$) and upper ($\varphi_{\max}$) limits of WT power factor angle. Equation (13) specifies that the probability of overvoltage at bus $j$ at hour $t$, $V_j^t$, should be lower than 2.5%. Equation (14) specifies that the probability of undervoltage at bus $j$ at hour $t$, $V_j^t$, should be lower than 2.5%. Consequently, $V_j^t$ is within the voltage limits [$V_{\min}$, $V_{\max}$] at a probability of

95% or higher. Such probabilistic constraints are in accordance with the requirements specified by the European Standard EN50160 [22]. Equation (15) states that the probability of overcurrent of branch $k$ at hour $t$, $I_k^t$, should be lower than 5%. In other words, $I_k^t$ is lower than the current limit of that branch $I_{k,\max}$ at a probability of 95% or higher. The probabilistic constraints of bus voltage and line current are further illustrated in Fig. 5.
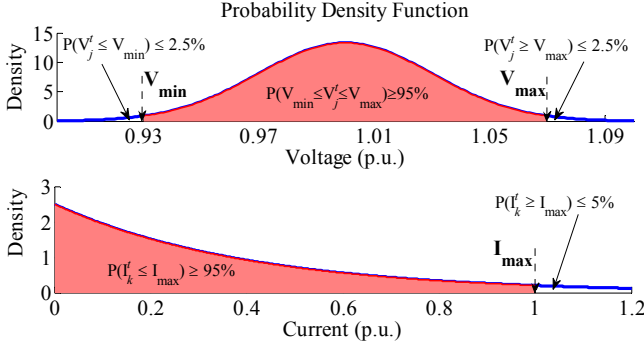


Fig. 5. Probabilistic constraints of bus voltage and line current.

The foregoing formulation, including (11)-(15), is a nonlinear constrained stochastic optimization problem. Therefore, a sequential quadratic programming implemented in the optimization toolbox of MATLAB [23] is combined with Monte Carlo simulation to find the optimal solution. Fig. 6 shows the flow chart of the stochastic optimization algorithm for each of the four periods. The algorithm mainly consists of three parts: time series simulation, probabilistic load flow calculation using Monte Carlo simulation, and nonlinear constrained optimization by sequential quadratic programming. The stop criteria of the optimization include first-order optimality measure and maximum number of iterations [23]. The optimization procedures are summarized as follows:

1) Simulate wind power and load time series from stochastic models and group the data into four periods and 24 hours,

2) Initialize WT power factor $\boldsymbol{\varphi}^t$ at hour $t$,

3) For each group of the data and given $\boldsymbol{\varphi}^t$, perform Monte Carlo simulation of length N to obtain probabilistic load flow results, which include the expectation of total system power losses, probability distribution of bus voltages and line currents,

4) Evaluate the objective function and the probabilistic constraints based on the probabilistic load flow results.

5) If the stop criteria are not reached, the sequential quadratic programming algorithm updates the WT power factor values $\boldsymbol{\varphi}^t$, and then go to step 3),

6) If any stop criterion is reached, terminate optimization at hour $t$. If $t$ is less than 24, $t = t + 1$ and go to step 2). Otherwise, output optimization results.

## IV. SYSTEM DESCRIPTION

This section describes the distribution system and data that are used to demonstrate the stochastic optimization problem formulated in section III for the optimal setting of WT power factors.
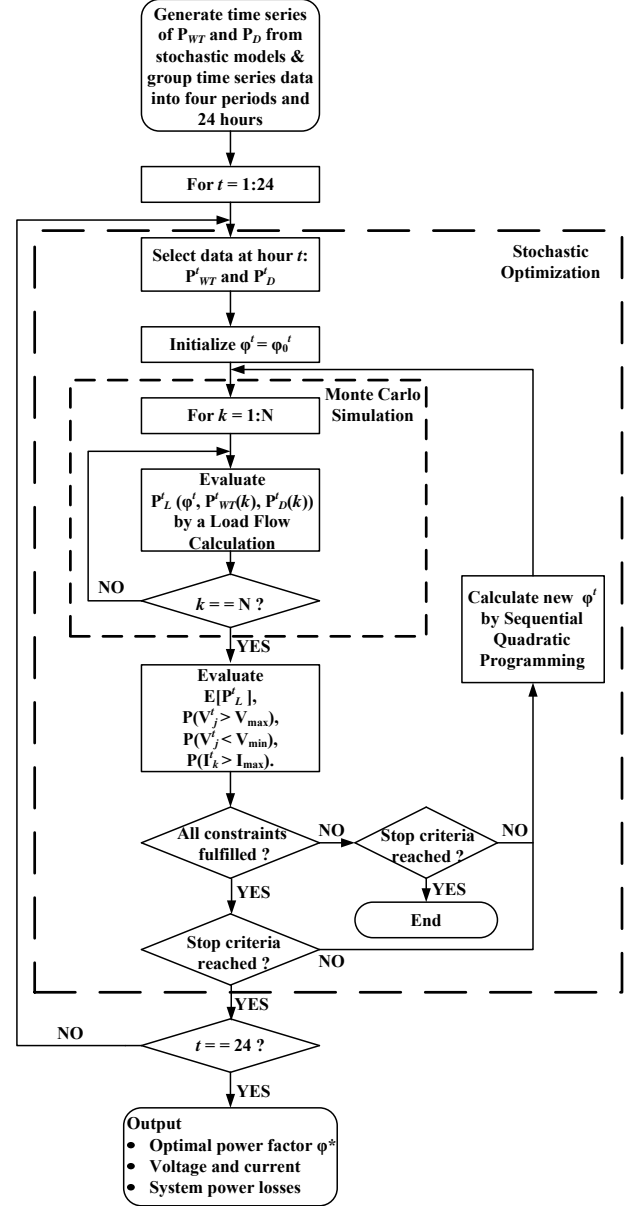


Fig. 6. Flow chart of the stochastic optimization algorithm for each of the four periods.

### A. Case Network

The case network is modified on the basis of the 69-bus radial distribution system in [24]. The modification consists of adding one 33/11 kV substation transformer and five WTs in the distribution system. These WTs are variable speed generators with power electronic interface, which can regulate their reactive power output to the grid. The configuration of the case network is shown in Fig. 7, with the network data provided in [24]. The case network has 70 buses in total. The capacity of the substation transformer is 12 MVA. The transformer is tap-regulated, with the voltage magnitude at the

low-voltage side controlled within [1, 0.9833] p.u. There are in total 13 tap positions, with maximum six steps above and six steps below the reference position. One tap step adjusts voltage by 0.0167 p.u. The voltage limits of all buses are set to ±7% of the nominal value (11 kV), i.e. $V_{max}$ = 1.07 p.u. and $V_{min}$ = 0.93 p.u. The current limit of all lines is 157A.

The network is divided into two areas. Area A consists of feeder F1 and F2 and area B consists of feeder F3 and F4. The two areas are located close to each other. Therefore, the cross-correlation between WPG in area A and WPG in area B is very strong.
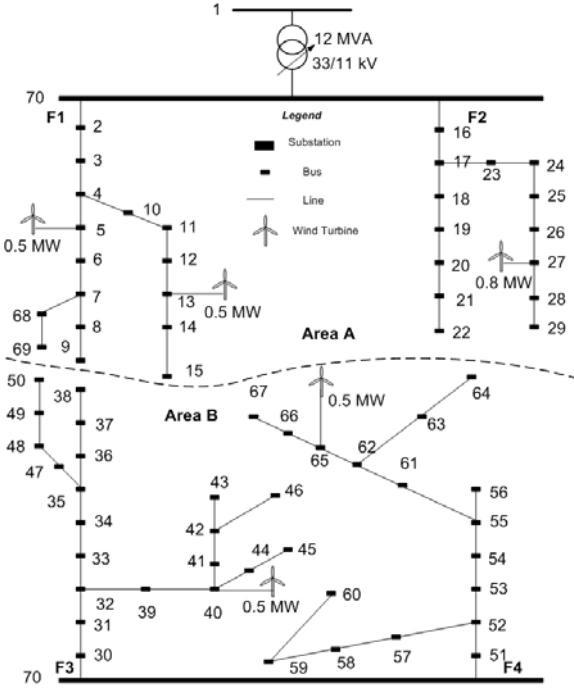


Fig. 7. The case network modified from the 69-bus distribution system [24].

### B. Wind Power Data

As shown in Fig. 7, there are in total five WTs connected to the network, with three WTs in area A (bus 5, 13 and 27 ) and two WTs in area B (bus 40 and 65). All the WTs have a capacity of 0.5 MW, but the one connected to bus 27, which is 0.8 MW. The WPG from the three WTs in area A is assumed to be fully correlated with each other. The full correlation is also assumed to the WPG from the two WTs in area B. Due to the close geography of area A and area B, WPG in area A is strongly correlated with WPG in area B. Such a strong cross-correlation is simulated using the bivariate-LARIMA model presented in section II. In order to account for the seasonal variations, the bivariate-LARIMA model is developed for the summer and winter period individually. The corresponding model parameters for the summer and winter period are summarized in the Appendix. On the basis of the model, bivariate wind power time series are simulated for a length of five years (43800 data points) for Monte Carlo simulations. Fig. 8 (a) shows the simulated bivariate wind power time series for a period of two weeks.

### C. Load Data

Load is connected to all the buses from bus 2 to bus 69. The peak load data at each bus are given in [24]. The total peak load of the network is (2.90 + j1.99) MVA. Full correlation is also assumed to the loads in area A as well as the loads in area B. The strong cross-correlation of the load in area A and the load in area B are caused by the diurnal period of the load as well as the similar temperature in the two areas. In this paper, the load model developed in [7] is adopted for the simulation. The model is based on an AR process and takes into account the seasonal variation, weekday/weekend and diurnal period of loads. Similarly, two load time series are simulated for a length of five years for Monte Carlo simulations. Fig. 8 (b) shows the two simulated load time series for a period of two weeks. The power factors of the loads are assumed time-invariant as provided in [24].
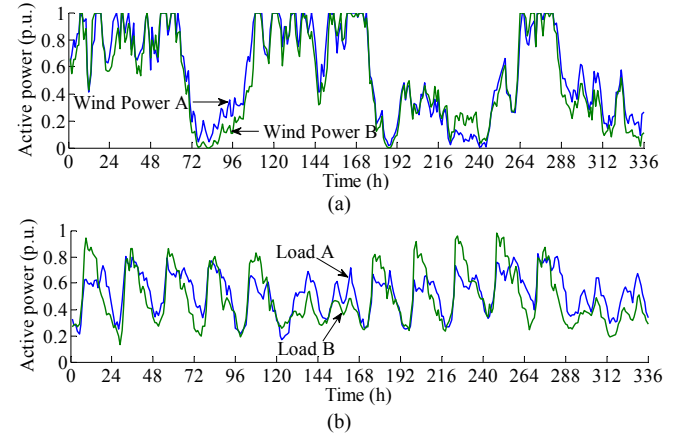


Fig. 8. Simulated time series of two weeks: (a) wind power generation, (b) load.

## V. SIMULATION RESULTS AND DISCUSSIONS

This section first presents the simulation results of the stochastic optimization of WT power factor. Then, the economic benefits of the optimal power factor setting are evaluated.

### A. Optimal Wind Turbine Power Factor Setting

Many countries, such as Denmark, Germany and the UK, specify power factor or reactive power generation requirement for grid-connected WTs [25]. The requirement varies from one country to another. For example, in the Danish grid code for grid-connected WTs, reactive power generation is confined to a control band with respect to active power generation. In practice, a grid-connected WT needs to fulfill the specific requirement depending on the regulation of the country. In this paper, the minimum power factor of WT is set to 0.8 both in leading and lagging directions. In other words, the maximum power-factor angle $\varphi_{max}$ is $37^0$ and the minimum power-factor angle $\varphi_{min}$ is $-37^0$. Normally, power-electronic converters of WTs are usually over-rated at 130% of the rated power output. Consider that apparent power equals to

$\sqrt{P^2+Q^2} = P^2\sqrt{1+\tan^2\varphi}$ . Such a power factor requirement ensures that at the rated active power output, the maximum apparent power output ($1\sqrt{1+\tan^2\varphi_{max}} = 125\%$) is within the converter rating.

Fig. 9 shows the optimal power factor angles of WTs obtained from the stochastic optimization for a summer weekday, a summer weekend, a winter weekday and a winter weekend. All the power factor angles are positive, which indicates that WTs generate reactive power. The power factor angles during a summer weekday are within [11, 32] degree, while the power factor angles during the other three periods are within [10, 24] degree. In addition, the power factor angles during a summer weekday fluctuate more frequently than during the other periods. This is caused by a relatively high wind power fluctuation in summer and a high load demand during weekdays. As shown in Fig. 9, it is also expected that the diurnal variation of load demand is reflected on the diurnal reactive power output of WTs.
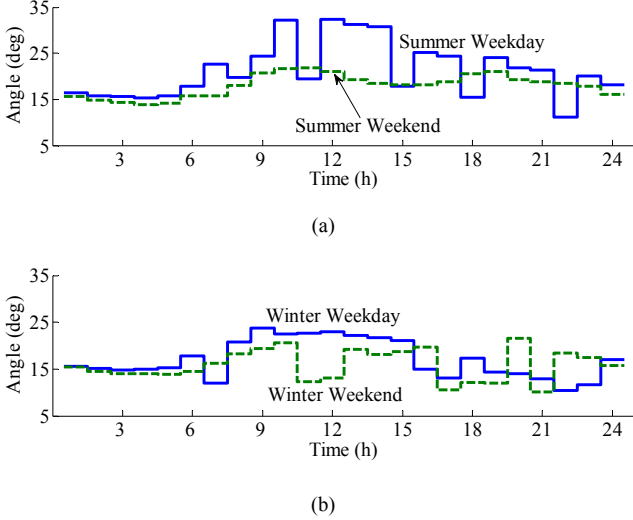


(a)



(b)

Fig. 9. Optimal daily power factor angles of WT at bus 27: (a) summer weekday and weekend, (b) winter weekday and weekend.

Fig. 10 shows the probability density function of the voltage at bus 27 over a year after the stochastic optimization. The mean value of the voltage is 0.99 p.u., and the standard deviation is around 2% of the mean value. In this case, the maximum allowed voltage (1.07 p.u.) is not exceeded. However, there is a bulge on the probability density function around 1 p.u. This is caused by the tap changer of the substation transformer, which regulates the voltage at bus 70 within [0.983, 1] p.u. As the WT is connected at bus 27, the voltage at 27 is on average slightly higher than the voltage at bus 70.

Fig. 11 shows the average daily power losses of the network during a summer weekday (SD), a summer weekend (SE), a winter weekday (WD) and a winter weekend (WE). The network power losses with WTs using unity power factor setting is shown on the first bin, and with WTs using optimal power factor setting shown on the second bin. The network power losses are lowered when using the optimal WT power factor setting. As compared to the case with unity power factor setting, the network losses are reduced by 10.4% during a summer weekday, 7.4% during a summer weekend, 16.7% during a winter weekday and 10.9% during a winter weekend. As a result, annual power losses are reduced approximately by 13% from 248 MWh with unity power factor of WTs to 215 MWh with optimal power factor setting of WTs. The significance of this amount of loss reduction will be evaluated in the following subsection.
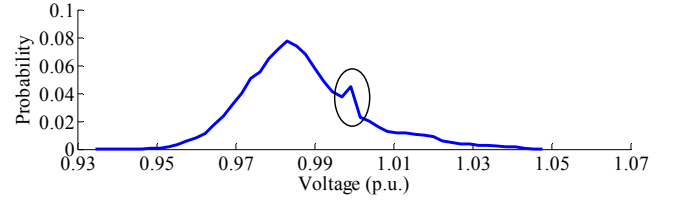


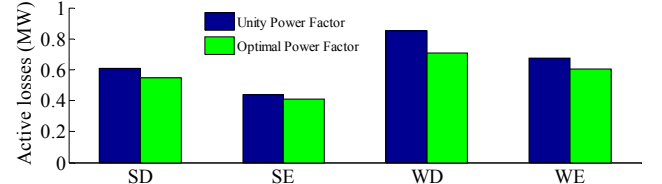Fig. 10. Empirical probability density function of voltage at bus 27.



Fig. 11. Network average daily power losses during a summer weekday (SD), summer weekend (SE), winter weekday (WD) and winter weekend (WE).

### B. Economic Benefits of Optimal Power Factor Setting

The loss reduction due to the optimal power factor setting of WTs may provide economic benefits to both network operators and WT owners. In order to evaluate such economic benefits, a cost assessment during the stage of system planning is carried out. The assessment is carried out over the period of twenty years of operation since the establishment of the system. For such a long-term system planning, the total assessed cost should include initial fixed costs, annual fixed costs and annual variable costs [26]. The initial fixed costs consist of a 33/11 kV 12 MVA tap-changing transformer, building cost, 33 kV and 11 kV switchgears, Petersen coil, assembling, and cable cost (20 km, XLPE three-core 150mm$^2$). Based on the price list provided by the local Danish DNO, these initial fixed costs are approximately 2.587 M€ in total. The annual fixed costs include the annual property tax, i.e. 3600 €, and annual maintenance and inspection cost, i.e. 6670 €. The above price values are provided by the Danish distribution network operator in Danish Krone (DKK) and are converted to € through the ratio of 7.50 DKK/€. The annual variable cost contains the electricity cost due to system power losses. Furthermore, system power losses may increase every year due to the annual load growth. A typical annual load growth rate is 1.5% for a Danish distribution system. Fig. 12 shows annual system power losses over twenty years with the 1.5% annual load growth rate. A fixed electricity price 70

€/MWh is used here to calculate the cost of power losses.

Consequently, for the initial year, the total investment costs, including the initial fixed costs and the property tax of the initial year, are 2.590 M€ (= 2.587 M€ + 0.0036 M€); the Maintenance and inspection costs are 6670 €. The annual power loss costs with unity and optimal power factor setting of WTs are listed in Table I. A present worth (PW) factor of 0.9 is used to evaluate the future money at the present value [26]. The network total cost is evaluated over twenty-year and summarized in Table I. As shown in Table I, the network total cost is 2.848 M€ when the unity power factor setting of WTs is used. However, the network total cost is reduced to 2.824 M€ when the optimal power factor setting of WTs is used. A total amount of 24000 € will be saved in this case. This saved money can be shared between the network operator and the WT owners.

Assume that WT owners are rewarded with all the savings obtained (24000 €). This amount of money can be offered by network operators to WT owners in two forms. One is annual cash payment, which is 1200 € per year. Another one is to reduce the energy transfer fee that network operators charge WT owners. This requires the following calculation of the energy transfer fee for WT owners. During a year, the total wind energy generated is 8841 MWh (for the total WT capacity of 2.8 MW). According to [26], the energy flow should also be discounted using the PW factor. Therefore, as shown in Table I, over a period of twenty years, the total wind energy generated is 77661 MWh. As a result, the energy transfer fee for WT owners is reduced by 0.03 cents/kWh (= 24000 € / 77661 MWh). Although this reduced energy transfer fee seems to be small, according to the local network operator, it actually can deplete the energy transfer fee by around 11% of what WT owners are paying at the moment (i.e. 0.28 cents/kWh). It is also worth mentioning that, for the above calculation, the optimal power factor setting is not updated every year even though the load grows annually. However, if the stochastic optimization is performed for every year considering annual load growth, a higher amount of annual system power losses can be achieved. Based on the above calculation, this will lead to a further reduction in total system costs and thus an even lower energy transfer fee for WT owners.
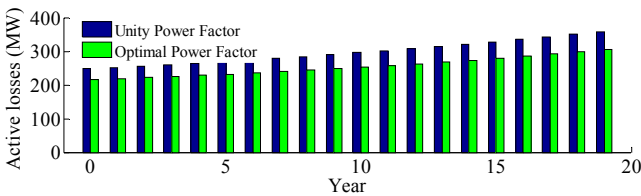


Fig. 12. Annual system power losses over 20 years with 1.5% annual load growth rate.

## VI. CONCLUSIONS AND FUTURE WORK

This paper has developed a multivariate-LARIMA model for correlated WPG. The multivariate-LARIMA model is obtained by introducing a cross-correlation structure to the LARIMA model. The cross-correlation structure models the correlation coefficients of WPG at different time lags adequately. Furthermore, the cross-correlation structure can be readily implemented. A sensitivity analysis of correlation coefficient indicates that as the cross-correlation of WPG weakens, the probability distribution of WPG becomes flatter.

Moreover, the proposed stochastic optimization algorithm provides optimal power factor settings of WTs for each hour of a day and for four types of days, i.e. a summer weekday, a summer-weekend day, a winter weekday and a winter-weekend day. As a result, a set of 96 power factor values is obtained for each of the WTs in the network. These power factor values considerably abate the system power losses under various combinations of WPG and load demand. In this case, an annual loss reduction of 13% is achieved. In light of the cost evaluation conducted, including the investment costs and operating costs of the network over a period of twenty years, the total costs are curtailed by 0.8%, which amounts to a saving of 24000 €. This amount of savings, if rewarded to the WT owners, may cut down the wind energy transfer fee by 11%.

The developed stochastic model and stochastic optimization can be used as a basic tool by network operators to estimate power losses of their networks and to negotiate with WT owners to achieve a more economic operation of the system.

As is evidenced in [18], the cross-correlation between WPG and load demand is very weak, ranging between 0 and 0.24. Thus, such a cross-correlation is not considered in this paper. However, the cross-correlation between WPG and load demand may become stronger through a new market mechanism. For instance, if a significant amount of wind power is traded in the electricity market, it will affect the variation of electricity price, which further influences system load behavior. Thus, future work can consider the cross-correlation between WPG and load demand in the stochastic models. The economic benefits of deferring system expansion because of increased maximum active power transfer capability can also be investigated. The multivariate stochastic wind power model developed in this paper can be used to represent wind farms in the reliability evaluation of a power system through a sequential Monte Carlo simulation [16], [17], [27]. If the outage rates of substation transformers, cables, circuit breakers and WTs are provided, the distribution reliability indices such as system average interruption frequency index (SAIFI), system average interruption duration index (SAIDI) and energy not supplied (ENS) can be computed accordingly [28].

## APPENDIX

The estimated model parameters of the bivariate-LARIMA(0,1,1) model shown in Fig. 1 are summarized as follows.

$$\hat{\boldsymbol{\theta}}_1 = \begin{bmatrix} \hat{\theta}_{11} & \hat{\theta}_{12} \\ \hat{\theta}_{21} & \hat{\theta}_{22} \end{bmatrix} = \begin{bmatrix} -0.15 & -0.04 \\ -0.44 & 0.22 \end{bmatrix}, \tag{16}$$

$$\hat{\boldsymbol{\Sigma}}_a = \begin{bmatrix} 0.62 & 0.56 \\ 0.56 & 0.61 \end{bmatrix}, \tag{17}$$

$$\hat{\boldsymbol{\theta}}_0 = \begin{bmatrix} \hat{\theta}_{0,1} \\ \hat{\theta}_{0,2} \end{bmatrix} = \begin{bmatrix} 0.008 \\ 0.007 \end{bmatrix}. \tag{18}$$

The model parameters $\boldsymbol{\theta}_1$ and $\boldsymbol{\Sigma}_a$ are calculated from the covariance matrices of the two measured wind power time series through:

$$\begin{cases} \boldsymbol{\theta}_1^2 \boldsymbol{\Gamma}(1) + \boldsymbol{\theta}_1 \boldsymbol{\Gamma}(0) + \boldsymbol{\Gamma}^T(1) = \mathbf{0} \\ \boldsymbol{\Gamma}(1) = -\boldsymbol{\Sigma}_a \boldsymbol{\theta}_1^T \end{cases}, \tag{19}$$

where $\boldsymbol{\Gamma}(0)$ is the covariance matrix at time-lag zero and $\boldsymbol{\Gamma}(1)$ is the covariance matrix at time-lag one. $\boldsymbol{\Gamma}(0)$ and $\boldsymbol{\Gamma}(1)$ are estimated from the measured wind power time series. Equation (19) is also valid for multivariate-LARIMA(0,1,1) model.

The model parameter $\boldsymbol{\theta}_0$ is adjusted to match the mean values of the simulated time series ($Y_1(t)$ and $Y_2(t)$) with the measured values through a Monte Carlo simulation.

When the bivariate-LARIMA model is applied to the summer and winter season individually, the corresponding model parameters are summarized as follows. For summer season,

$$\hat{\boldsymbol{\theta}}_{1,\mathrm{sm}} = \begin{bmatrix} -0.18 & 0.01 \\ -0.46 & 0.25 \end{bmatrix},$$

$$\hat{\boldsymbol{\Sigma}}_{a,\mathrm{sm}} = \begin{bmatrix} 0.68 & 0.61 \\ 0.61 & 0.65 \end{bmatrix},$$

$$\hat{\boldsymbol{\theta}}_{0,\mathrm{sm}} = \begin{bmatrix} -0.03 \\ -0.04 \end{bmatrix}.$$

For winter season,

$$\hat{\boldsymbol{\theta}}_{1,\mathrm{wt}} = \begin{bmatrix} -0.11 & -0.10 \\ -0.42 & 0.18 \end{bmatrix},$$

$$\hat{\boldsymbol{\Sigma}}_{a,\mathrm{wt}} = \begin{bmatrix} 0.56 & 0.51 \\ 0.51 & 0.56 \end{bmatrix},$$

$$\hat{\boldsymbol{\theta}}_{0,\mathrm{sm}} = \begin{bmatrix} 0.04 \\ 0.05 \end{bmatrix}.$$

TABLE I
TWENTY-YEAR EVALUATION OF THE NETWORK INVESTMENT AND OPERATING COST ($10^3$ €)

| Study Year | Invest. | Maint. & Insp. | Loss Cost | | Annual Cost | | PW Factor | Discount Cost | | Wind Energy (MWh) |
|---|---|---|---|---|---|---|---|---|---|---|
| | | | Unity | Opt. | Unity | Opt. | | Unity | Opt. | |
| 0 | 2590 | 6.67 | 17.4 | 15.1 | 2614 | 2612 | 1.000 | 2614 | 2612 | 8841 |
| 1 | 3.6 | 6.67 | 17.4 | 15.3 | 27.9 | 25.6 | 0.900 | 25.1 | 23.0 | 7957 |
| 2 | 3.6 | 6.67 | 17.9 | 15.5 | 28.2 | 25.8 | 0.810 | 22.8 | 20.9 | 7161 |
| 3 | 3.6 | 6.67 | 18.2 | 15.8 | 28.5 | 26.0 | 0.729 | 20.8 | 19.0 | 6445 |
| … | … | … | … | … | … | … | … | … | … | … |
| 19 | 3.6 | 6.67 | 25.1 | 21.4 | 35.4 | 31.6 | 0.315 | 4.8 | 4.3 | 2785 |
| Total | 2658.4 | 133.4 | 415 | 356 | 3207 | 3148 | | **2848** | **2824** | **77661** |
| **Total wind energy transfer fee reduced is (2848-2824) × $10^3$ € / 77661 MWh = 0.03 cents/kWh** | | | | | | | | | | |

REFERENCES

[1] IEA, "Renewable energy: Market & policy trends in IEA countries," International Energy Agency (IEA), 2004. Available: http://www.iea.org/textbase/nppdf/free/2004/renewable1.pdf

[2] EWEA, "Wind now leads EU power sector," The European Wind Energy Association (EWEA), 2009. Available: http://www.ewea.org/fileadmin/ewea_documents/documents/press_releases/2009/02_February_2009_Wind_now_leads_EU_power_sector.pdf

[3] T. Ackermann, *Wind Power in Power Systems*. Chichester: John Wiley & Sons, 2005.

[4] X. Ding, W. Lee, J. Wang and L. Liu, "Studies on stochastic unit commitment formulation with flexible generating units," *Electric Power Systems Research*, vol. 80, pp. 130-141, 2010.

[5] U. Aytun Ozturk, M. Mainak and B. A. Norman, "A solution to the stochastic unit commitment problem using chance constrained programming," *IEEE Trans. Power Syst.,* vol. 19, pp. 1589-1598, Aug. 2004.

[6] P. Kall and S. W. Wallace, *Stochastic Programming*. Chichester: John Wiley & Sons, 1994.

[7] P. Chen, B. Bak-Jensen, and Z. Chen, "Probabilistic load models for simulating the impact of load management," *IEEE PES General Meeting 2009*, Calgary, Canada, Jul. 2009.

[8] G. Desrochers, M. Blanchard and S. Sud, "A Monte-Carlo simulation method for the economic assessment of the contribution of wind energy to power systems," *IEEE Trans. Energy Convers.*, vol. EC-1, pp. 50-56, Dec. 1986.

[9] R. Billinton, H. Chen and R. Ghajar, "Time-series models for reliability evaluation of power systems including wind energy," *Microelectron. Reliab.*, vol. 36, pp. 1253-1261, 1996.

[10] R. Karki and R. Billinton, "Cost-effective wind energy utilization for reliable power supply," *IEEE Trans. Energy Convers.*, vol. 19, pp. 435-440, Jun. 2004.

[11] P. Chen, T. Pedersen, B. Bak-Jensen and Z. Chen, "ARIMA-based time series model of stochastic wind power generation," accepted for future publication in *IEEE Trans. Power Syst.* Paper ID TPWRS-00365-2009.

[12] F. Castro Sayas and R. N. Allan, "Generation Availability Assessment of Wind Farms," *IEE Proc. Generation, Transmission, Distribution*, vol. 143, pp. 507-518, Sep. 1996.

[13] N. B. Negra, O. Holmstrøm, B. Bak-Jensen and P. Sørensen, "Model of a synthetic wind Speed time series generator," *Wind Energy*, vol. 11, pp. 193-209, 2008.

[14] G. Papaefthymiou and B. Klöckl, "MCMC for wind power simulation," IEEE Trans. Energy Conversion, vol. 23, pp. 234-240, Mar. 2008.

[15] G. Papaefthymiou, *Integration of Stochastic Generation in Power Systems*. PhD Dissertation, Delft University of Technology, Delft, 2007.

[16] R. Billinton and W. Wangdee, "Reliability-based transmission reinforcement planning associated with large-scale wind farms," *IEEE Trans. Power Syst.,* vol. 22, pp. 34-41, Feb. 2007.

[17] W. Wangdee and R. Billinton, "Considering load-carrying capability and wind speed correlation of WECS in generation adequacy assessement," *IEEE Trans. Energy Convers.*, vol. 21, pp. 734-741, Sep. 2006.

[18] G. Papaefthymiou and D. Kurowicka, "Using copulas for modeling stochastic dependence in power system uncertainty analysis," *IEEE Trans. Power Syst.*, vol. 24, pp. 40-49, Feb. 2009.

[19] W. W. S. Wei, *Time Series Analysis: Univariate and Multivariate Methods*. Redwood City: Addison-Wesley, 1990.

[20] H. Saadat, *Power System Analysis*. 2nd ed. Singapore: McGraw Hill, 2002.

[21] R.A. Jabr and B.C. Pal, "Intermittent wind generation in optimal power flow dispatching" *IEE Proc. Generation, Transmission, Distribution*, vol. 3, pp. 66-74, Sep. 2009.

[22] EN 50160, "European Standard for Voltage Characteristics of Electricity Supplied by Public Distribution Systems," *European Committee for Electrotechnical Standardization* (CENELEC), Brussels, pp. 14, Nov. 1999.

[23] Mathworks, *MATLAB Optimization ToolboxTM 4, User's Guide*, 2009, Available: http://www.mathworks.com/access/helpdesk/help/pdf_doc/optim/optim_tb.pdf

[24] D. Das, "A fuzzy multiobjective approach for network reconfiguration of distribution systems," *IEEE Trans. Power Del.*, vol. 21, pp. 202-209, Feb. 2006.

[25] UNIFLEX PM, "Converter applications in future European Electricity Network.," pp. 123–161, Aug. 2007. Available: http://www.eee.nottingham.ac.uk/uniflex/Documents/W2_AU_DV_2001_B.pdf

[26] H. L. Willis and W. G. Scott, *Distributed Power Generation: Planning and Evaluation*. Boca Raton: CRC Press, 2000.

[27] R. Billinton and G. Bai, "Generating capacity adequacy associated with wind energy," *IEEE Trans. Energy Convers.*, vol. 19, pp. 641-646, Sep. 2004.

[28] R. Billinton and R.N. Allan, *Reliability Evaluation of Power Systems*. 2nd ed. New York: Plenum Press, 1996.

## VII. Biographies

**Peiyuan Chen** (S'2007, M'2010) received his B.Eng. degree in Electrical Engineering from Zhejiang University, China, in 2004 and M.Sc. degree in Electric Power Engineering from Chalmers University of Technology, Sweden, in 2006. From August of 2005 to June of 2006, he was also with ABB Corporate Research, Sweden. He is currently pursuing his Ph.D. degree at Aalborg University, Denmark. He is working on the probabilistic modeling of power systems with integration of renewable energy based distributed generation. His focus is on stochastic models of wind power generation and their applications in power system operation and planning.
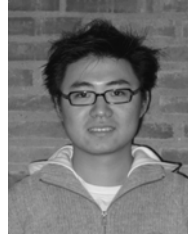
**Pierluigi Siano** got the M.Sc. degree in Electronic Engineering and the Ph.D. in Information and Electrical Engineering both from the University of Salerno. Since 2001, he has been Assistant Professor at the Department of Electrical and Information Engineering of the University of Salerno.
His research activity focuses on application of soft computing methodologies to power system analysis and planning.
He was scientific coordinator of the research project: "Integration of New and Renewable Energy into Urban Electrical Networks" supported by the British-Italian partnership programme for young researchers (2005-2006).
He served as reviewer and session chairman for many international conferences. Dr Siano is a Chartered Engineer and has authored more than 60 papers mainly in international journals and conferences in the fields of power systems.

**Birgitte Bak-Jensen** (M'1988) received her M.Sc. degree in Electrical Engineering in 1986 and a Ph.D. degree in "Modelling of High Voltage Components" in 1992, both degrees from Institute of Energy Technology, Aalborg University, Denmark. From 1986-1988 she was with Electrolux Elmotor A/S, Aalborg, Denmark as an Electrical Design Engineer. She is an Associate Professor in the Institute of Energy Technology, Aalborg University, where she has worked since August 1988. Her fields of interest are modelling and diagnosis of electrical components, power quality and stability in power systems. During the last years, integration of dispersed generation to the network grid has become one of her main fields, where she has participated in many projects concerning wind turbines and their connection to the grid.

**Zhe Chen** (M'1995, SM'1998) received the B.Eng. and M.Sc. degrees from Northeast China Institute of Electric Power Engineering, Jilin City, China, and the Ph.D. degree from University of Durham, U.K. He was a Lecturer and then a Senior Lecturer with De Montfort University, U.K. Since 2002, Dr. Chen became a Research Professor and is now a Professor with the Department of Energy Technology, Aalborg University, Denmark. He is the coordinator of Wind Power System Research program at the Institute of Energy Technology, Aalborg University. His background areas are power systems, power electronics and electric machines; and his main current research areas are wind energy and modern power systems. Dr Chen has more than 190 publications in his technical field. He is an Associate Editor (Renewable Energy) of the IEEE Transactions on Power Electronics. Dr. Z. Chen is a Member of the Institution of Engineering and Technology (London, U.K.), and a Chartered Engineer in the U.K.